Orissa Journal of Physics
ISSN 0974-8202

Vol. 27, No.1
February 2020
pp. 27-35

Optimised patterns for square solar cells with tabs for better cell efficiency

R M PUJAHARI[1, *], S K RATHA[2], C K DAS[2] and M C ADHIKARY[2]

[1]*ABES Institute of Technology, Ghaziabad, India*
[2]*Dept. of Applied Physics and Ballistics, F M University, Balasore, India*
[*]*Corresponding author, E-mail: rpujahari@gmail.com*

Received: 28.11.2019 ; Revised : 17.12.2019 ; Accepted : 9.1.2020

Abstract. The metallisation pattern for the front side for a typical crystalline silicon solar cell with screen printed metallisation. In this paper a 12.5 x 12.5 cm^2 cell with two tabs is considered. The finger distance s for a H-grid pattern with our procedure. During the process it has been observed that the smeared out metallisation has uniform thickness and is characterised by a single parameter. The optimal pattern is determined by the cell geometry, the location of the interconnections of the pattern to the tabs, the irradiance condition for the maximum power point like $V_{mpp} J_{mpp}$, the characteristics of metallisation technique.

Keywords. H-grid metallisation pattern, smeared out metallisation, shadow fraction, series resistance.

1. Introduction

A solar cell is a photodiode which is used to convert light energy into electrical energy and it thereby serves as a source of d.c. power under illumination. Usually a solar cell(e.g. silicon solar cell) consists of a thick p-layer(base) and a thin n-layer (emitter) on the top forming a shallow p-n junction. Light penetrates through the emitter layer (the front surface) to the base generates excess minority carriers which is made to flow through a load via the metal contacts to the front and back surface of the cell. If we look at the front surface we can easily access that the two dominating source of loss in cell efficiency [1.2] are

i. The shadowing or optical loss due to coverage of a part of the surface by metal contact lines.
ii. The resistive losses due to carrier flow in the emitter layer, semiconductor-metal contact and in the metal contact lines.

If the front surface of the entire cell is covered with a metal layer, the optical loss will be maximum and the resistive loss will be minimum but no power can be taken out of the solar cell.

Metallisation patterns are essential component of many solar cells. They are applied on both rear and front side of the solar cell to make electrical contacts to the cell. As an example through screen printing any pattern can be printed. Optimisation of patterns can be done with a class of patterns of certain topology. The most common example of optimisation of fingers is done in H-grid metallisation pattern [3,4].

The great majority of crystalline silicon solar cells have a metallisation pattern at the front side and H-grid pattern is one of them. The pattern consists of wide strips of metallization called busbars [5]. The fingers are the narrow lines of metallisation perpendicular to the busbars. For most large area industrial silicon solar cells the busbars and fingers are deposited in one step by screen printing. A tab is soldered on the top of each busbar [6]. The tabs serve two main functions like electrical connections to the other cells in the module and to provide extra conductivity to the bus bar.

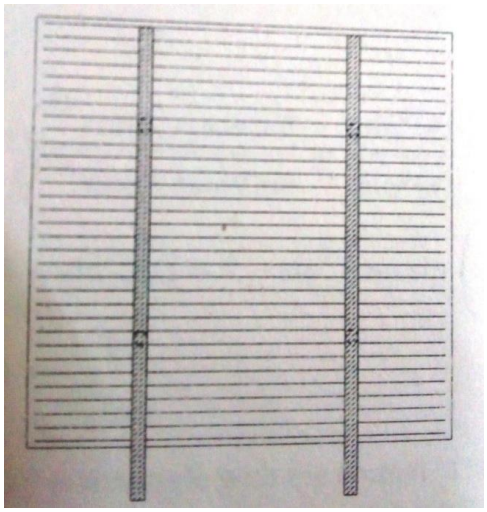

Fig. 1. An H-grid metallisation pattern. The pattern consists of two solder joints per tab at locations indicated by the dotted oval.

2. Principle of the design method

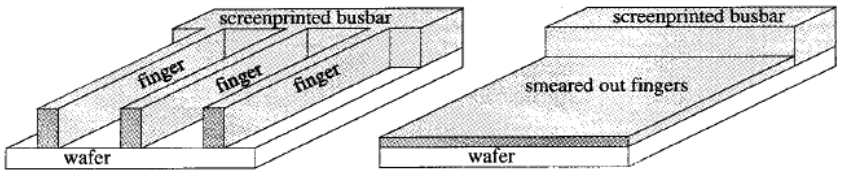

Fig. 2.1. Smearing of the metallisation of a set of parallel fingers. Left: fingers Right: smeared out fingers

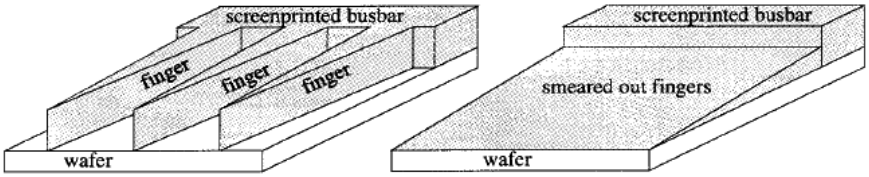

Fig. 2.2. Smearing of the metallisation of a set of parallel tapered fingers. Left: fingers Right: smeared out fingers

Figure 2.1 and 2.2 illustrate the principle of the method with the help of a few fingers of an H-grid pattern[7]. The metallisation in the fingers of this pattern is smeared out perpendicularly to the direction of the fingers. The smeared out metallisation covers the complete cell[8].

In order to maintain the right overall transparency we assign to the full metallisation in this case of uniform transparency of 75%. In the case of the design as illustrated in Fig 2.2 the transparency assigned to the smeared out metallisation decreases linearly from 100% at the tip of the finger to 50% at the intersection at the busbars [9]. This transparent smeared out metallisation differs from the fingers in one aspect that is it can conduct current in any direction while the ordinary uniform fingers cannot. This extra degree of freedom is used to optimise the solar cell metallisation design further.

The central idea of the design of the pattern of metallisation is divided into two steps. Firstly the designing and optimisation has been carried out on the right hand sides as shown in Fig. 2.1 and 2.2. Secondly the transparent smeared out metallisation is converted into a line pattern with exactly same series resistance and transparency by reversing the process of smearing out the metallisation.

Therefore the optimisation can be achieved with a minimum number of parameters (typically 10). Therefore full optimisation of the smeared out metallisation is possible[10].

The second step is just a translation step and is necessary only after transparent smeared out metallisation has been optimised. The series resistance is unchanged as by the translation step as the orientation of fingers is chosen parallel to the current flow. And the cross section of the metallisation is not changed.

In a transparent smeared out metallisation no emitter losses occur and the contact resistance is lower than in a pattern because of the full coverage.

3. Mathematical method

The screen printed metallisation is characterised by its thickness d_0, its sheet resistance $\rho_{sm,0}$ and the minimum width w that can be achieved during printing. The transparent smeared out metallisation is thinner than the final screen printed metallisation and it is characterised by its position dependent thickness $d(x,y)$. The sheet resistance $\rho_{sm}(x,y)$ and the transparency of the transparent smeared out metallisation, the higher its sheets resistance and transparency are[11].

The shadow fraction $P_s(x,y)$ in the screen printed metallisation is directly linked to the ratio of smeared out metallisation and the screen printed metallisation.

$$P_s(x,y) = d(x,y)/d_0 \quad (1)$$

The transparent smeared out metallisation is thinner than the final screen printed metallisation and consequently it has a higher sheet resistance.

$$P_{sm}(x,y) = \rho_{sm,0} d_0/d(x,y) = \rho_{sm,0}/d(x,y) \quad (2)$$

We assume that local current J_{mpp} and voltage V_{mpp} at maximum power point are given. Optimisation of yearly yield can be achieved by using a single yearly averaged current J_{mpp} and voltage V_{mpp} [11].

The total power P_g that could be produced by the solar cell without shadow and resistance losses is given by the following integral over the cell surface S.

$$P_g = \int_S J_{mpp}\, V_{mpp}\, dxdy \quad (3)$$

However there are shadow- and resistive losses. On the illuminated side of the cell the current density the J_{mpp} is reduced to the shadowing by the opaque metallisation.

$$J'_{mpp}(x,y) \;=\; J_{mpp}\,(1 - P_s(x,y)\quad) \tag{4}$$

The voltage $V(x,y)$ in the metallisation is determined by solving a partial differential equation across the cell surface:

$$\nabla\left(\frac{1}{\rho_{sm}(x,y)}\nabla V(x,y)\right) = \; -J'_{mpp}(x,y) \tag{5}$$

The differential equation must be completed with boundary conditions. The boundary conditions are a prescribed voltage at the connections to the external leads. Across other boundaries no current flow is possible. The current flow pattern resulting from the solution of this differential equation is the pattern that gives the least ohmic dissipation[12].

From the voltage $V(x,y)$ and the current vector $j(x,y) = \frac{1}{\rho_{sm}(x,y)}\nabla V(x,y)$ in the metallisation and the power $P_m$dissipated in the metallisation can be calculated:

$$P_m = \int_S \left|\frac{1}{\rho_{sm}(x,y)}\nabla V(x,y)\right| dxdy \tag{6}$$

The transparent smeared out metallisation covers the entire cell surface. Therefore contact resistances are much smaller than in final pattern and no emitter sheet resistance losses occur. During optimisation of the transparent smeared out metallisation the losses like sheet resistance losses and increased contact resistance losses must be taken care[13].

The contact between emitter and metallisation results in a contact resistance loss P_c and is characterised by a contact resistance ρ_c. The dissipation due to contact resistance is inversely proportional to the coverage fraction $P_s(x,y)$. The lower the coverage, the higher the dissipation[14,15].

$$P_c = \rho_c \int_S \frac{J'_{mpp}(x,y)2}{P_s(x,y)}dxdy \tag{7}$$

In order to calculate the loss P_c due to emitter sheet resistance we make the assumption that everywhere the pattern consists locally of metallisation lines running in parallel. In this way we get for P_c and P_e expressions [16,17]

$$\begin{aligned} P_e &= \int_S \left(\frac{S(x,y)2}{12}(1 - P_s(x,y))\rho_e J'_{mpp}(x,y)^2 dxdy\right. \\ &= \int_S \left(\frac{w^2}{12}\left(\frac{1-P_s(x,y)}{P_s(x,y)2}\right)\rho_e J'_{mpp}(x,y)^2 dxdy\right. \end{aligned} \tag{8}$$

Here w^2 is the finger width that we can achieve and $S(x,y)$ is the distance between the fingers. The power loss to the shadowing is written as:

$$P_s = \int_S P_s(x,y) J_{mpp}\, V_{mpp}\, dxdy \tag{9}$$

The total loss $P_t = P_s + P_m + P_c + P_e$ is a combination of the shadow loss and the resistive losses. $P_s(x,y)$ can be optimised numerically by considering P_t as a function of $P_s(x,y)$. [18]

3. Results and Discussion

To illustrate the method we consider a front side metallisation for a screen printed 10 x 10 cm^2 multicrystalline silicon solar cell with two tabs.

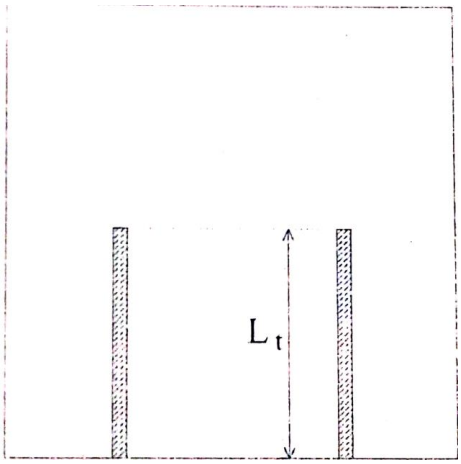

Fig. 3. Interconnection geometry for optimisation pattern. The tab length L_t is optimised.

The Figure 3 shows the interconnection geometry considered. We want to optimise the tab length and design the finger pattern for maximum yearly yield. We will compare this with a standard H-grid pattern with optimised finger distance. In all cases screen printed busbars are present under the tabs with the same dimensions as the tabs. In order to optimise the tab length it suffices to analyse the transparent smeared out metallisation. The translation to a line pattern only has to be done for the optimal tab length, where one is interested in the actual pattern. The tab can be modelled straightforwardly by a region with fixed sheet resistance[19]

Table 1: Comparison of different metallisation patterns for the front side.

Pattern	**Tab length**	**P_s(%)**	**R_{sc}(mΩ)**	**Loss(%)**
H- grid	10 cm	8.0	8.7	10.6%
Optimised	10 cm	7.8	9.2	10.5%
Optimised	8.5 cm	7.2	9.5	10.1%
Optimised	7.0 cm	6.9	10.4	10.0%
Optimised	3.3 cm	7.2	16.4	12.1%

Table 1 show the results of different metallisation patterns. A tab length around 7.0 cm is optimal in this case. If the tab gets much shorter the resistance in the fingers increases, if the tab becomes longer they cause increasing shadow losses without decreasing the resistance much[20].

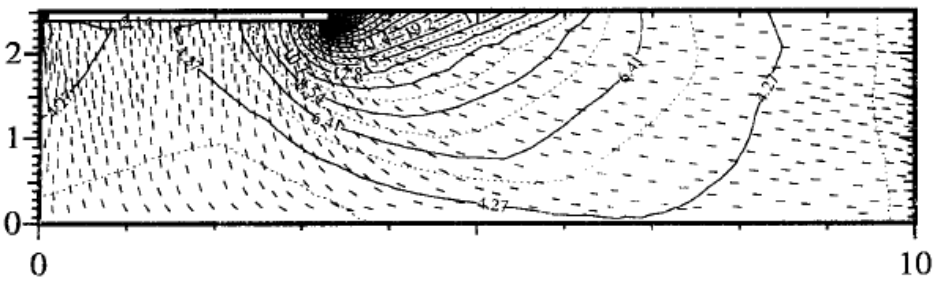

Fig. 4. Superposition of current vectors and contour plot of coverage fraction for a tab length of 3.3 cm

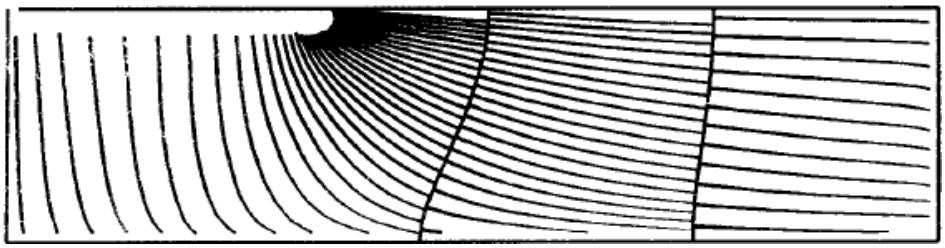

Fig. 5. Pattern derived from fig 4. Finger widths have been multiplied with 4 for improved quality.

Figure 4 shows the transparent smeared out metallisation resulting from step 1 of our method in the form of contour plot. For reasons of symmetry it was sufficient to analyse the quarter of the cell. The current vectors have all been normalised to the same length to make direction of current flow more clearly

visible. Fig. 5 shows a metallisation pattern consistent with the data from Fig. 4. The metallisation fingers are aligned with the current vectors. They have been tapered in order to achieve the right coverage fraction. The optimisation procedure results in a more dense metallisation pattern towards the end of the tab.

4. Conclusion

We conclude that a method has been designed and developed for the optimisation of metallisation patterns. No pre-assumption on the topology of the pattern is made. The optimal pattern can be determined by the cell geometry, the location of the interconnections of the pattern to the tabs, the irradiance condition for the maximum power point like $V_{mpp} J_{mpp}$, the characteristics of metallisation technique.

The optimal patterns can be introduced in a screen printing line without extra cost so they may be a variable alternative to standard pattern.

Acknowledgements

The authors express their sincere thanks to P.G. Dept. of Applied Physics and Ballistics, FM University, Balasore, India and ABES Institute of Technology, Ghaziabad for continuous stimulation and support for the present research.

References

[1] R J Handy, *Solid State Electronics*, **10**, 765 (1967)

[2] A Flat and A G Milnes, *Solar Energy*, **23**, 289 (1979)

[3] H B Serreze. *Optimizing solar cell performance by simultaneous consideration of grid pattern design and interconnect configurations*. Proceedings of the 13th *IEEE PVSC*. pp. 609-614, 1978.

[4] G De Mey and P De Visschere, *Nieuw archief Wiskunde*, **IV(1)**, 270 (1983).

[5] S H El-hefnawi and H H Afifi, *Front layer design optimisation for photovoltaic solar cell under concentrated nonuniform sunlight*, Proc. *5th Int. PVSEC*, pp. 609–614, 1978.

[6] T A Gessert, X Li and T J Coutts, *Solar Cells*, **30**, 459 (1991)

[7] A R Burgers, J A Eikelboom and H H C de Moor, *Optimisation of metallisation patterns for yearly yield*. In *26thIEEE Photovoltaic Specialists Conference, Anaheim*, pp 219-222. IEEE, 1997. ECN-RX-97-061.

[8] M A Green, Solar Cells: Operating Priciples, *Technology and System Applications, 1986 Ed.*

[9] M F Stuckings and A W Blankers, *Solar Energy Materials and Solar Cells*, **59(3)**, 233 (1999)

[10] W Neu, A Kress, W Jooss, P Fath and J Nijs, *Solar Energy Materials and Solar Cells*, **57(2)**, 179 (1999)

[11] S Bouridas, G Beaucarne, A Slaoui, J Poortmans, B Semanche and C Dubois, *Solar Energy Materials and Solar Cells*, **65(1-4)**, 487 (1992)

[12] U Gangopadhyaya, K Sinha and H Saha, *Indian J. of Phys*. **61A**, 266 (1987)

[13] E Vazsonyi, Z Vertesy, A Toth and J Szlufcik, *Journal of Micromechanics and Microengineering*, **13**, 165 (2003)

[14] U Gangopadhyay, S K Dhungel, P K Basu, S K Dutta, H Saha and Junsin Yi, *Solar Energy Materials and Solar Cells*, **91**, 285 (2007)

[15] Munesh Chandra Adhikary, Rakesh Mohan Pujahari, *Journal of Energy and Power Resources.ISSN:Print-2333-9136,*Online-2333-9144(2014)

[16] P K Basu, R M Pujahari, H. Kaur, Devi Singh, D Varandani and B R Mehta, *Solar Energy,* **84**, 1658 (2010)

[17] R M Pujahari and M C Adhikary, *ISST Journal of Applied Physics, ISSN:0976-903X*, **5(1)**, (2014)

[18] Devi Singh, R M Pujahari, Harpreet Kaur and P K Basu *ISST Journal of Applied Physics.ISSN:0976-903X,* **1(2)**, 9 (2010)

[19] R M Pujahari, M C Adhikary, 12th *International Congress on Renewable Energy (ICORE-2014), ISBN: 978-81-8454-150-2*, Manekshaw Centre, New Delhi, Organised by Solar Energy Society of India, December 8-9, p.251-254, 2014

[20] M C Adhikary, R M Pujahari *International Congress on Renewable Energy (ICORE-2013), ISBN: 978-93-82880-80-6,* KIIT University, Bhubaneswar, Organised by Solar Energy Society of India, November 27-29, p.181-186, 2013